The effects of composition and thermal treatment on the magnetic properties of $Fe_{100-x}Co_x$ nanowire arrays based on AAO templates

LIN CAO, XINPING QIU*
Department of Chemistry, Tsinghua University, Beijing 100084, Beijing, P.R. China
E-mail: qiuxp@mail.tsinghua.edu.cn
E-mail: caolin@mail.tsinghua.edu.cn

JINGBO DING, HULIN LI
Department of Chemistry, Lanzhou University, Lanzhou, Gansu 730000, Gansu, P.R. China

LIQUAN CHEN
Department of Chemistry, Tsinghua University, Beijing 100084, Beijing, P.R. China

Published online: 3 March 2006

A series of $Fe_{100-x}Co_x$ nanowire arrays with about 6.0 μm in length and 60 nm in diameter have been fabricated successfully by AC deposition of Fe and Co atoms into anodic aluminum oxide (AAO) templates. Samples with different composition could be obtained by adjusting the concentration ratio of Fe^{2+} and Co^{2+} in the solution of the electrolyte. The composition of the samples were determined by atomic absorption spectroscopy. Structural analysis was performed using scanning electron microscopy and X-ray diffraction. The magnetic properties of the samples were examined by vibrating sample magnetometry. The effects of composition and thermal treatment on the magnetic properties of the nanowire arrays have been examined. XRD shows that the nanowires have a body-centred-cubic (bcc) structure with a preferred orientation of the <110> axis parallel to the nanowires. When x is between 80 and 90, nanowires undergo a phase transformation $\alpha \rightarrow \gamma$ which is very different from Fe–Co bulk alloy. Furthermore, a localized magnetization reversal mechanism of the nanowire arrays was conformed. It is also found that the magnetic properties of the arrays are critically dependent on the compositions and thermal treatment. With suitable choices of these factors, a kind of soft ferromagnetic film can be produced while maintaining a high coercivity and squareness.

1. Introduction

Fe–Co alloys exhibit high saturation magnetization M_s ($M_s \approx 2.4$ T) and high Curie temperatures T_c($T_c \approx 900^\circ$C) that make them very important as potential candidates for high temperature applications [1–3]. But without the addition of other elements such as Cr, Fe-Co films can not be used as magnetic recording material as the magnetocrystalline anisotropy K_1 of the ordered FeCo alloys is neglectable [4]. However, this is changed drastically owing to the appearance of Quantum Magnetic Disk (QMD) [5] proposed based on nanostructure fabrication technique.

Physical and chemical properties of substances can be considerably altered when they are exhibited on a nanoscopic scale. Nanoscience and nanotechnology are not simply a miniaturization in sizes, but an in-depth revolution in physical concepts, system design, materials synthesis and manufacturing [6, 7]. One important characteristic of QMD is a non-continuous self-magnetized moment, and without applied field each discrete unit (bit) remains only two possible and steady magnetization states: up or down. More important, the direction of each magnetic moment and the coercivity can be controlled by changing the structure of micropores and the size of particles. With isolated, needle-like magnetic elements uniformly embedded in a nonmagnetic disk, such large area nano-scale arrays have attracted more attention because discrete magnetic recording schemes may overcome thermal stability and noise limits of conventional

*Author to whom all correspondence should be addressed.
0022-2461
DOI: 10.1007/s10853-006-7181-8

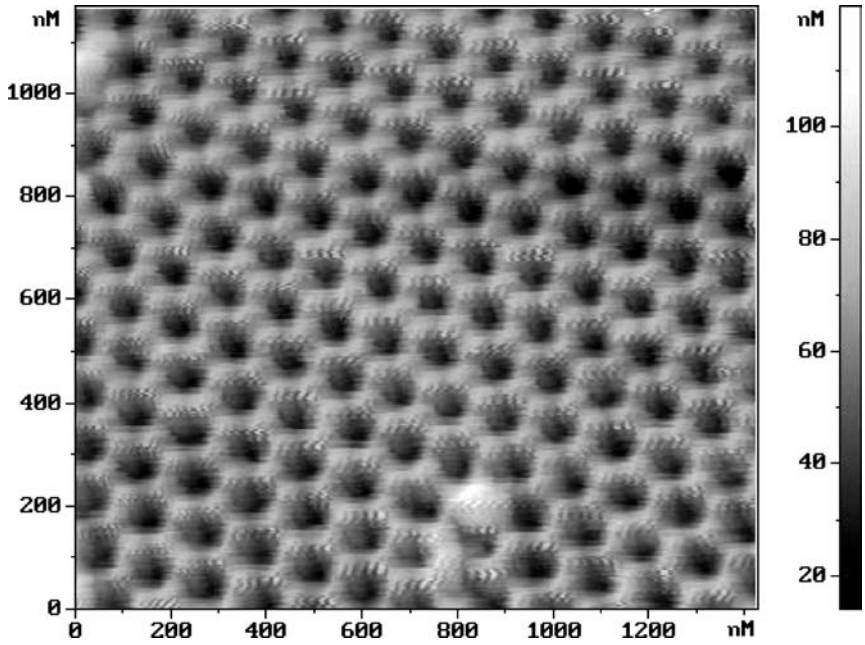

Figure 1 AFM image of AAO template prepared by two-step anodization.

TABLE I The compositions of $Fe_{100-x}Co_x$ nanowires prepared with various concentrations of $CoSO_4 \cdot 7H_2O$ and $FeSO_4 \cdot 7H_2O$.

Sample no.	$Fe_{90}Co_{10}$	$Fe_{80}Co_{20}$	$Fe_{70}Co_{30}$	$Fe_{60}Co_{40}$	$Fe_{50}Co_{50}$	$Fe_{40}Co_{60}$	$Fe_{30}Co_{70}$	$Fe_{20}Co_{80}$	$Fe_{10}Co_{90}$
Concentration of $CoSO_4 \cdot 7H_2O$ (g/l)	12.0	24.0	36.0	46.0	60.0	72.0	84.0	96.0	108.0
Concentration of $FeSO_4 \cdot 7H_2O$ (g/l)	108.0	96.0	84.0	72.0	60.0	48.0	36.0	24.0	12.0
Co content in solution (%)	10.0	20.0	30.0	40.0	50.0	60.0	70.0	80.0	90.0
Co content in $Fe_{100-x}Co_x$ (%)	4.2	13.2	23.3	33.1	42.3	51.6	62.2	71.8	81.8

hard disk media and can reach a higher magnetic storage density. Furthermore, due to the high aspect ratio of nanowires, magneto-crystalline anisotropy is not a predominant factor, as in the bulk phase or in thin films. The strong magnetic anisotropy in the localized nanowire arrays is mainly predominated by shape anisotropy with the easy axis parallel to the nanowires. The shape anisotropy of the magnetic nanowires can be estimated by coherent rotation mechanism ($K_s = (\mu_0/4)M_s^2$) [8]. Recently magnetic nanowires and their periodic arrays have attracted much attention due to the novel physical and chemical properties that are different from the bulk. They show possible applications in high-density magnetic media and as sensors [9–12]. Due to the high M_s in FeCo alloys, high K_s can be obtained and the magnetic properties are dominated by shape anisotropy. Compared with other materials, Fe-Co nanowire arrays show excellent perpendicular magnetic anisotropy and are promising for magnetic recording.

Because the pore density is high ($10^9 \sim 10^{12}/cm^2$); the distribution of the pores is uniform; the diameter of the pores is small (4∼200 nm) and can be easily controlled, anodic aluminum oxide (AAO) is considered as a particularly attractive template for fabricating nanowires [13]. Ferromagnetic nanowire arrays prepared by the AAO technique show distinct magnetic properties, such as easy axis of magnetization perpendicular to the substrate plane, enhanced coercivity H_c and remanent magnetization M_r [14]. To date, Fe [15], Co [16], Ni [17], FeNi [18], CuCo [19] and other magnetic nanowire arrays have been fabricated and their magnetic properties have been studied systematically.

In this paper, we systematically report the preparation, microstructure and the effects of composition and annealing on magnetic properties of $Fe_{100-x}Co_x$ nanowire arrays by AC electro-deposition into nanoporous anodic aluminum oxide (AAO) templates. More important, basing on our previous work [20] we further explain the microstructure and magnetic characteristic of $Fe_{100-x}Co_x$ nanowire arrays on the view of crystal structure, micro-electric theory and magnetization reversal mechanism.

2. Experimental procedures

Ordered AAO templates with pore diameter about 60 nm (see Fig. 1) were prepared by anodic oxidation of 99.999% Al sheets (30 mm × 18 mm) in 0.3 M $C_2H_2O_4$ aqueous solution at 40 V (DC) for an hour at 15°C under two-step anodizing process. The preparation process of AAO was described in detail in previous work done by the others

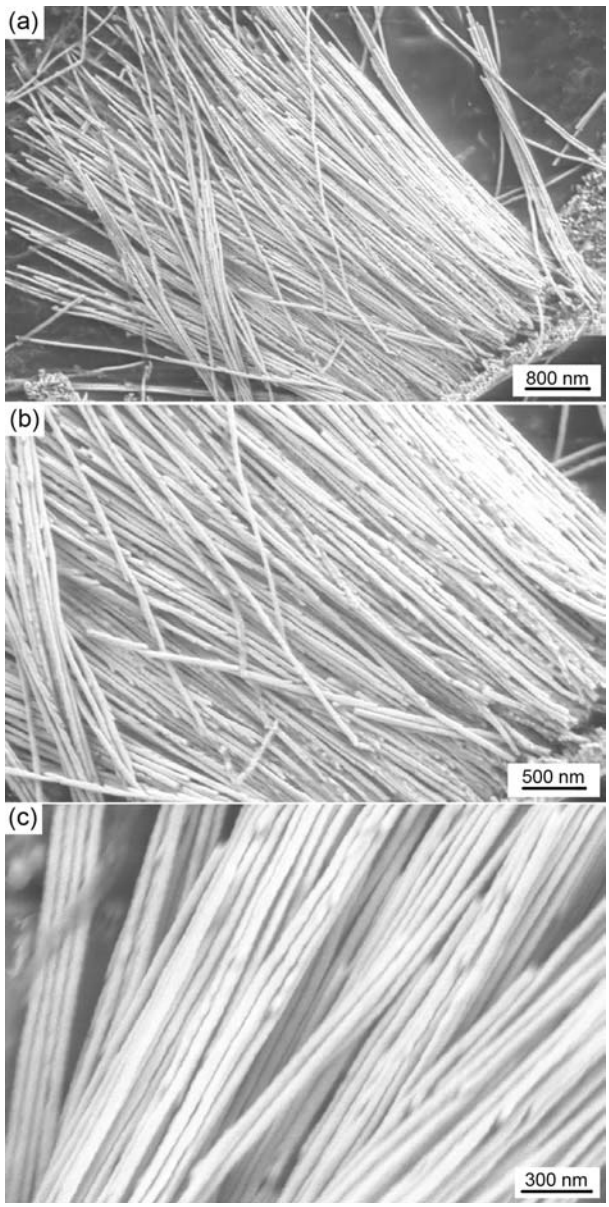

Figure 2 SEM images of $Fe_{40}Co_{60}$ nanowire arrays taken at different magnification with AAO template removed.

in my old lab [21, 22] and anywhere else [13]. The AAO were characterized by the atomic force microscopy (P-47-SPM-MDT). $Fe_{100-x}Co_x$ ($x = 0-100$) nanowire arrays were fabricated by co-electrodepositing Fe and Co into AAO templates. A graphite and an AAO template with aluminum substrate served as the counter electrode and working electrode, respectively. The electrolyte solution used in electro-deposition consisted of 12–108 g/l $CoSO_4 \cdot 7H_2O$, 12–108 *g*/l $FeSO_4 \cdot 7H_2O$, boric acid (30 *g*/l) and ascorbic acid (1.5 g). Boric acid was added to make the deposition easier, and ascorbic acid was used as an inhibitor to prevent the oxidation of Fe^{2+} to Fe^{3+}. The pH value of the electrolyte was maintained at 3–4. All the electro-depositions were carried at the frequency of 200 Hz. The deposition potential is about 11.5 V (AC) at 25°C, and the time of all electro-depositions is 1 min. The samples were numbered according to the value of $CoSO_4 \cdot 7H_2O$ and $FeSO_4 \cdot 7H_2O$ concentration (seen Table I).

The composition of the samples were determined by atomic absorption spectroscopy (AAS; Hitachi, 180-80), the structural characterizations were performed by means of X-ray diffraction (XRD; Rigaku, Model D/max 2400, Cu Ka radiation, $\lambda = 1.54184$ Å), the microstructures of $Fe_{100-x}Co_x$ nanowires were investigated by scanning electron microscopy (SEM; LEO-1530), the magnetic properties of the samples were examined by vibrating sample magnetometer (VSM; Japan, VSM-5s-15).

To obtain the SEM image of the as-deposited nanowire array, the sample was dipped into a mixed acid solution containing 3.5 vol% H_3PO_4 and 45 g/l $HCrO_3$ at 30°C for 30 min to dissolve the AAO template partly. AAO films filled with $Fe_{100-x}Co_x$ nanowires were exfoliated from the Al substrates using saturated $HgCl_2$ solution for the XRD test.

3. Results and discussion

3.1. The compositions of the samples

The AAS analysis data were listed in Table I. From this table, even if the Fe concentration is in direct proportion to that of Co always more 7–8% Fe than Co are found, which indicates that it is more difficult to electro-deposit Co^{2+} into AAO than Fe^{2+}probably due to higher stabilization constant of Co coordination complex than that of Fe. Considering the kinetic characteristic of this system, the electro-deposition velocity of Fe^{2+} or Co^{2+} is strongly controlled by the migratory velocity of Fe^{2+} or Co^{2+}, which is related to the radius of ions. Because the radius of hydrated ions of Fe^{2+} and Co^{2+} are almost equivalent, the migratory velocity of Fe^{2+} is almost the same as that of Co^{2+}. Accordingly, the value of Fe concentration is in direct proportion to that of Co in our prepared $Fe_{100-x}Co_x$ nanowires. So, the compositions of $Fe_{100-x}Co_x$ nanowires are controlled by the relative ratio of Fe^{2+} and Co^{2+}, and can be adjusted by varying the ratio of Fe^{2+} and Co^{2+} in the electrolyte.

3.2. Morphology and structural properties

Fig. 2 shows the SEM images of different amplification for Fe-Co nanowires with the AAO templates dissolved completely. As showed in these figures, the microstructures of all the nanowires differ little from one another, with about 6.0 μm (Fig. 2a) in length and 60 nm (Fig. 2c) in diameter. Selected electron diffraction photo shows that the prepared nanowires are composed by many multiple-crystal particles. This multi-microcrystalline structure is possible because Fe-Co alloy particles are deposited rapidly into pores only every half AC period rather than long continuous growth process during AC electro-deposition.

Fig. 3 shows the X-ray diffraction (XRD) spectra of $Fe_{100-x}Co_x/Al_2O_3$ nanowire arrays. From the graphs it is obvious that in the range of $0 < x < 80$, the diffraction peaks can be assigned to FeCo (110) and amorphous AAO ($2\theta < 40^\circ$), and some graphs also show a weak FeCo

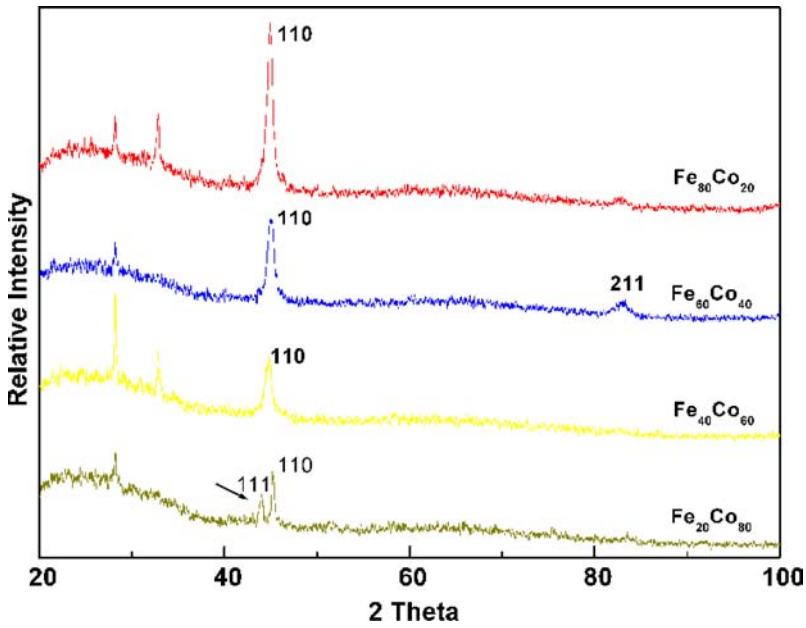

Figure 3 Powder Cu-KÁ XRD spectra of $Fe_{100-x}Co_x/Al_2O_3$ nanowire arrays with four Fe components.

(211) peak (indicated by an arrow). The microstructures of $Fe_{100-x}Co_x$ nanowires are very different from those of bulk Fe-Co alloy. In the nanowire arrays the peak of FeCo (110) is very strong, which indicates that the nanowires have a body-centred-cubic (bcc) structure with a (110) preferred orientation rather than bcc-FeCo (100) preferred in the Fe-Co bulk alloy. Furthermore, when x is between 73 and 90, besides bcc-FeCo (110) structure the graph also shows a fcc-Co (111) peak. This means that the $Fe_{100-x}Co_x$ nanowires undergo a phase transformation from α (bcc-FeCo) to γ (bcc-FeCo and fcc-Co). In bulk Fe-Co alloy the phase transformation $\alpha \rightarrow \gamma$ occurs at 73% Co. So we can conclude that in the nanowires the phase transformation takes place at the higher concentration of Co.

3.3. Magnetic properties

3.3.1. Effect of composition

The control of composition is often a key element in optimizing the magnetic properties for a magnetic material, whether for bulk or for thin film form. It has been seen in many systems that slight variation of the composition can cause substantial changes in the coercive and anisotropic properties. Iron cobalt is a well-known example of a magnetic material that exhibits significant variation of magnetic properties with composition. In our work a series of samples with different components could be obtained easily by merely adjusting the relative concentration of Fe^{2+} and Co^{2+} in the electrolyte.

The dependence relations between the coercivity H_c, squareness (M_r/M_s) and the Co content of the $Fe_{100-x}Co_x$ alloy arrays are shown in Fig. 4a. The samples were measured with an applied field (10 kOe) parallel and perpendicular to the wire axis at room temperature. When the applied field is parallel to the wire axis, with the concentration of Co increasing, the coercivity H_c(//)and squareness (M_rM_s) increase and reach the maxima of $H_c = 2200$ Oe, $M_r/M_s = 1$ (corresponding to Co concentration of 73%). Then both drop drastically with the continuous increase of x. The change of coercivity with the Co content is the result of the microstructure change of the nanowires and the reasons can be explained tentatively as follows: for d-group transition metals, such as iron-cobalt, the density of 4s and 3d electrons are the two main factors that affect the charge density near the iron nuclei. Table II shows the valence electron distributions in 4s and 3d electron energy belts of Fe and Co. The 4s electrons give no contribution to magnetic properties, but they can affect the distribution in 3d energy belt. From the data in Table II it can be seen that Fe with the positive and negative spin belts have cavities. When Co is added into Fe, with the increase of Co the cavity sum in the positive belt decreases while the cavity sum in the negative belt increases. So the total magnetic moment increases and coercivity H_c also linearly increases with the Co content increasing. But in fact, due to rapid deposition into AAO template of Fe^{2+} and Co^{2+}, there are big stress and many defects in the nanowires, which result in the appearance of disordered structure bcc-FeCo (211) that has a negative K_1 and decrease H_c. Furthermore, during the phase transformation $\alpha \rightarrow \gamma$ the Co (111) of the face-centred-cubic (fcc) structure, whose saturation magnetism is smaller than that of bcc-FeCo (110), appears in the range of $x > 80$. These are the main reasons that result in the drastic drop of coercivity H_c in the range of $x > 80$. When the applied field is perpendicular to the nanowire arrays, the coercivity H_c and squareness M_r/M_s of the $Fe_{100-x}Co_x$ alloy arrays are much smaller ($H_c < 700$ Oe, $M_r/M_s < 0.2$), and changes are small according to Co content x.

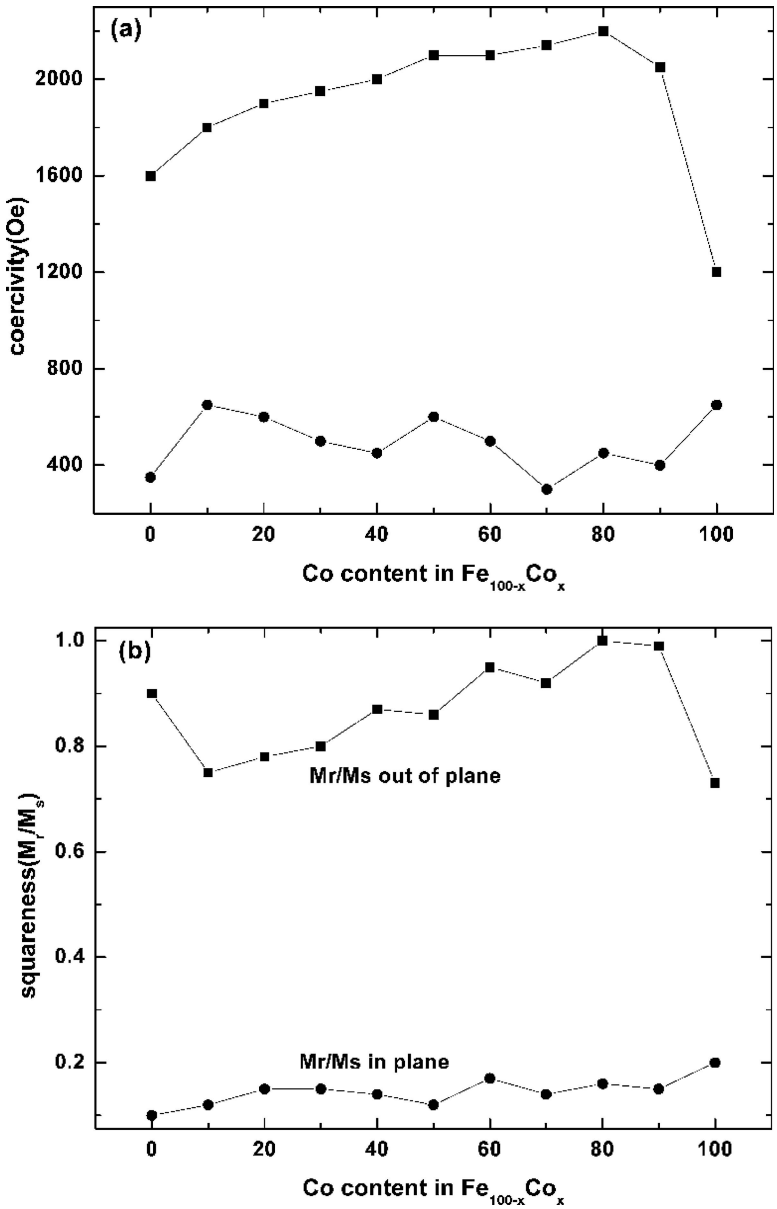

Figure 4 The dependence relations between the coercivity H_c (a), squareness M_r/M_s (b) and the Co content in the $Fe_{100-x}Co_x$ alloy arrays:(//) external field parallel to nanowire axis; (⊥) external field perpendicular to nanowire axis: (a) coercivity H_c vs. Co content of the $Fe_{100-x}Co_x$ alloy arrays; (b) squareness M_r/M_s vs. Co content of the $Fe_{100-x}Co_x$ alloy arrays.

TABLE II The valence electron distribution in 4s and 3d energy belts of Fe and Co

		Electron distribution according to energy belt theory				The sum of the unfilled cavity		
Element	Electron configuration	$3d^+$	$3d^-$	$4s^+$	$4s^-$	$3d^+$	$3d^-$	The effective spin sum
Fe	$3d^64s^2$	4.8	2.6	0.3	0.3	0.2	2.4	2.2
Co	$3d^74s^2$	5.0	3.3	0.35	0.35	0	1.7	1.7

3.3.2. Effect of annealing

In order to check for annealing effects on $Fe_{100-x}Co_x$ nanowire arrays, all the samples are annealed at different temperatures 300, 400, 450, 500, 550 and 600°C, respectively with a pressure of 10^{-3} Pa in Ar atmosphere. It has been found that the coercivities of the nanowire arrays with different amount of Fe and Co significantly increase. The effect of annealing temperature of some samples on coercivitiy was examined in Fig. 5a. When the annealing temperature is between 300°C and 500°C a clear increase in coercivity can be observed. Further increases in temperature show a reduction in the coercivity past the

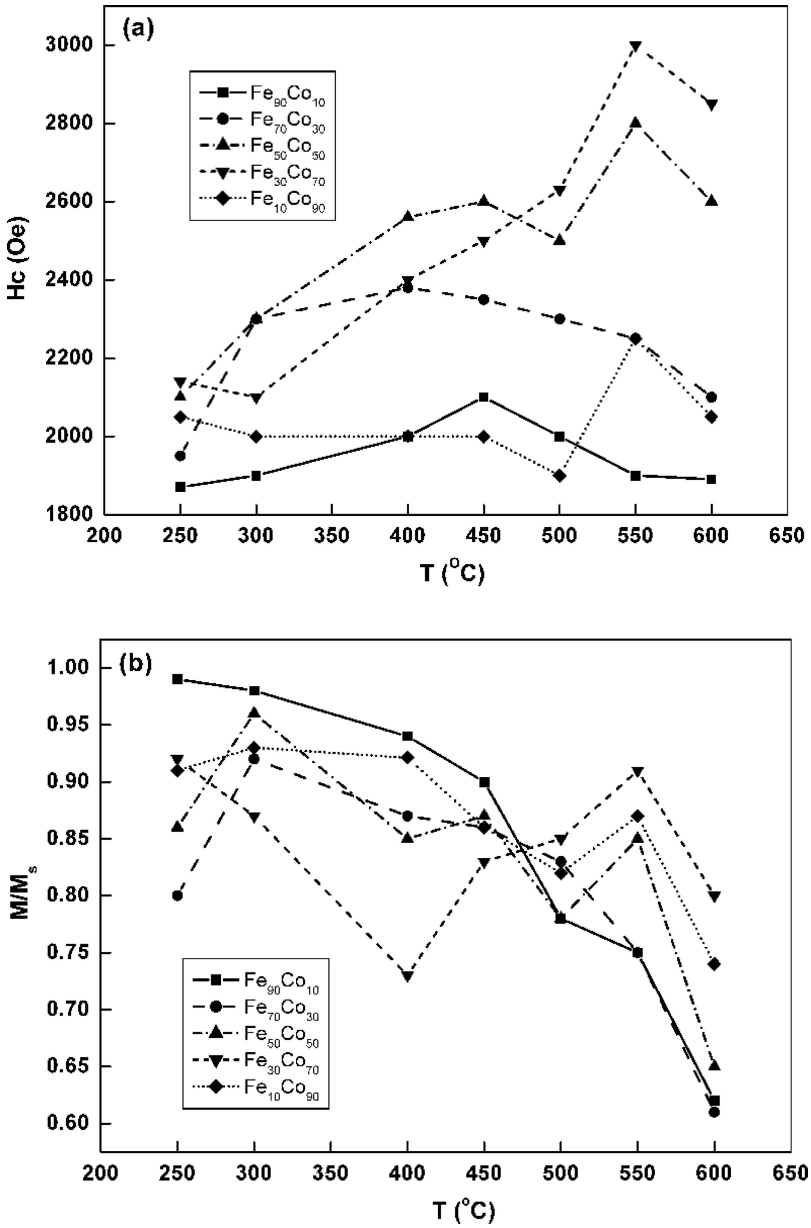

Figure 5 The relations between the coercivity H_c, squareness M_r/M_s and the annealing temperatiure: (a) the relations between the coercivity H_c and the annealing temperatiure; (b) the relations between the squareness M_r/M_s and the annealing temperature.

temperature limit of 550°C. It has been also found that the squareness of almost all the samples (Fig. 5b) decreases with annealing temperature. At low annealing temperature and high Co content, M_r/M_s of the samples stays almost constant at a very high level (about 0.75). As Fe content increases, the squareness drops down rapidly to a very low value of 0.6. All samples showing the lowest squareness (below 0.7) were obtained for those samples annealed at the highest temperature. In addition, a coercivity as high as 3000 Oe and squareness about 0.91 can be obtained in $Fe_{30}Co_{70}$ annealed at 550°C, the coercivity of which is much higher than that of Fe (1600 Oe), Co (1200 Oe) or its as-prepared state (2200 Oe).

The increase in coercivity after annealing is related to microstructure change during the annealing process. Firstly, there is a sort of internal stress in the as-deposited samples induced by rapid deposition of Fe^{2+} and Co^{2+}. Thermal annealing relieves the internal stress and a high degree of crystallinity is obtained. So the M_s of annealed sample is higher than its as-deposited state, as the sequence high H_c is expected. Secondly, there is a large mismatch of the thermal expansion coefficients (α) between $Fe_{100-x}Co_x$ alloy and alumina. Because the α (about 14.0 $\times$ 10^{-6} K^{-1}) of FeCo alloy is much higher than that of AAO (about 6.0 $\times$ 10^{-6} K^{-1}), FeCo alloy tends to expand along the wire axis during annealing and form a columnar structure with easy axis along nanowire arrays, which will improve shape anisotropy at local region.

For samples with high Fe content, the reason of the decrease in coercivity and the reduction in

squareness can be explained as follows: due to Fe/Co short-range order, there are microscale changes such as the change of K_1 (the first magneto-crystalline anisotropy) and phase segregation during the annealing process, which will enhance uniaxial anisotropy perpendicular to nanowire arrays and decrease H_c and M_r/M_s in the alloy arrays. In addition, at high temperature Fe atoms in the nanowire arrays will react with oxygen existing in AAO template and form Fe oxide, which decreases the saturation magnetization M_s and perpendicular anisotropy.

3.4. Magnetization reversal mechanism

The principal origin of perpendicular anisotropy is due to the competition between magnetocrystalline anisotropy and shape anisotropy. In this case, because the aspect ratio of $Fe_{100-x}Co_x$ nanowire is very high (about 20), the strong magnetic anisotropy found in the localized $Fe_{100-x}Co_x$ alloy arrays is mainly dominated by shape anisotropy with the easy axis parallel to nanowires. Furthermore, when the applied field is parallel to the wire axis the magnitude of coercivity H_c is tied up with magnetization reversal mechanism of the nanowire arrays. According to coherent rotation mechanism ($K_s = (\mu_o/4) M_s^2$) proposed by Stoner and Wohlfarth (SW model) [12], the process of magnetization reversal is coherent rotation to infinitely long ideal nanowires and the corresponding anisotropy field $H_c \approx H_A = 2K_u/M_s = M_s/2$. In the case of $Fe_{100-x}Co_x$, M_s is about 1.5∼2.4 T so coercivity, H_c, is estimated to be about 1800–3800 Oe. However, a real magnetic nanowire is far more complicated than a collection of impendent SW particles due to various kinds of imperfection in the wire and the influence of magnetostatic interactions between wires. This approach significantly overestimates the coercivity of the wires, and recently localized nucleation mode has been proposed by Skomski *et al*. [13, 23] which is in view of polycrystalline structure of the wires and magnetization perturbances associated with wire-thickness fluctuations, crystalline defects, impurities and geometrical features at the wire ends. The localization of the nucleation mode is accompanied by a coercivity reduction. Based on the research of Skomski *et al*., the corresponding coercivity could be expressed as [23]:

$$H_C = 2K_{eff}/\mu_0 M_s - \alpha^2 \Delta K^2/(2A\mu_0 M_s)$$
$$= \mu_0 M_s/2 - \alpha^2 \Delta K^2/(2A\mu_0 M_s)$$

Where A is the exchange stiffness, K_{eff} is effective uniaxial anisotropy determined by magnetocrystalline anisotropy and shape anisotropy, α is the length which determines the defect's volume and ΔK is the reduced local anisotropy (via the localization length $R_L/\alpha\Delta K$) accompanied by an easy-axis misalignment. By means of the formula one can rationalize H_c values of 20–30% of H_A (anisotropy field, $H_A = \mu M_s/2$), as often observed. In the case of $Fe_{100-x}Co_x$, M_s is about 1.5–2.4 T so H_c is estimated to be about 1800 Oe∼3800 Oe. This is in good agreement with our experimental results (in our work H_c is in the range of 1800–2200 Oe, when $x = 10$–90). So localized reversal model is very appropriate to explain the reversal process in our serial $Fe_{100-x}Co_x$.

4. Conclusions

To summarize, highly ordered $Fe_{100-x}Co_x$ ($x = 0$–100) alloy nanowire arrays have been fabricated systematically and successfully by AC electro-deposition into hexagonal nanoporous anodic aluminum oxide (AAO) templates. Bcc structure with a <110> preferred orientation was obtained in as-prepared samples. Composition and annealing could influence the coercivity and squareness of the $Fe_{100-x}Co_x$ nanowire arrays. It was found that high coercivity ($H_c = 2200$ Oe) and squareness ($M_r/M_s = 1.0$) could be obtained when the Co content x is about 80. When the annealing temperature is about 500°C, the coercivity and squareness as high as 3000 Oe and 0.91 could be obtained respectively. We also found that magnetic microstructure and intrinsic stress affected the coercivity of the as-prepared samples largely and the reversal mechanism should be nucleation-propagation reversal mechanism. The magnetic easy axis of Fe_xCo_{1-x} arrays was mainly determined by the competition between the shape anisotropy and the magneto-crystalline anisotropy of the nanowires. As $Fe_{100-x}Co_x$ nanowire arrays showed superior perpendicular magnetic anisotropy, they present a great potential for high-density magnetic recording.

Acknowledgments

The authors acknowledge the financial support of the National Key Basic Research and Development Program (2002CB211803).

References

1. A. GONZ'ALEZ and A. HERNANDO, *Phys. Rev.* **B 65** (2002) 094432.
2. R. H. YU, S. BASU, Y. ZHANG and J. Q. XIAO, *J. Appl. Phys.* **85** (1999) 6034
3. H. MOUMENI, S. ALLEG, C. DJEBBARI and F. Z. BENTAYEB, *J. Mater. Sci.* **39** (2004) 5441
4. R. M. BOZORTH, "Ferromagnetism." IEEE, New York, 1991.
5. S.Y. CHOU, *IEEE Trans. Magn. MAG.* **85** (1997) 652
6. E. C. STONER and E. P. WOHLFARTH, *Phil. Trans. R. Soc.* **A 240** (1948) 599
7. C. N. R. RAO, G. U. KULKARNI, P. J. THOMAS and P. P. EDWARDS, *Chem. Eur. J.* **8** (2002) 29
8. Z. L. WANG, *Adv. Mater.* **15** (2003) 1497
9. S. Y. CHOU, M. S. WEI, P. R. KRAUSS and P. B. FISCHER, *J. Vac. Sci. Tech. B* **12** (1994) 3695
10. M. HEHN, K. OUNADJELA, J. BUCHER, F. ROUSSEAUX, D. DECANINI, B. BARTENLIAN and C. CHAPPERT, *Science* **272** (1995) 1782
11. H. MASUDA and K. FUKUDA, *Science* **268** (1995) 1466
12. D. MISHRA, S. ANAND, R.K. PANDA and R.P. DAS, *Mater. Chem. Phys.* **86** (2004) 132
13. D. J. SELLMYER, M. ZENG and R. SKOMSKI, *J. Phys. Condens. Matter.* **13** (2001) R433

14. H. R. KHAN and K. PETRIKOWSKI, *J. Magn. Magn. Mater.* **249** (2002) 458
15. Y. PENG, H. L. ZHANG, S. L. PAN and H. L. LI, *J. Appl. Phys.* **87** (2000) 7405
16. H. ZENG, M. ZHENG, R. SKOMSKI and D. J. SELLMYER, *J. Appl. Phy* **87** (2000) 4718
17. M. ZHENG, L. MENON, H. ZENG, Y. LIU, S. BANDYOPADHYAY, R. D. KIRBY and D. J. SELLMYER, *Phys. Rev. B* **62** (2000) 12282
18. H. R. KHAN and K. PETRIKOWSKI, *Mater. Sci. and Eng. C* **19** (2002) 345
19. L. BELLIARD, J. MILTAT, A. THIAVILLE, S. DUBOIS, J. L. DUVAIL and L. PIRAUX, *J. Magn. Magn. Mater.* **190** (1998) 1
20. D. H. QIN, Y. PENG, L. CAO and H.L. LI, *Chem. Phys. Lett.* **374** (2003) 661
21. S. L. PAN, D. D. ZENG and H. L. LI, *Appl. Phys. A* **70** (2000) 637
22. C. W. WANG, Y. PENG, S .L. PAN and H. L. LI, *Acta. Phys. Sin.* **11** (1999) 2146
23. R. SKOMSKI, H. ZENG and D. J. SELLMYER, *J. Magn. Magn. Mater.* **249** (2002) 175

Received 10 May
and accepted 5 July 2005